X-Ray Scattering Study of Smectic Ordering in a Silica Aerogel

Noel A. Clark,[1] Tommaso Bellini,[1,2] Rainer M. Malzbender,[1] Britt N. Thomas,[1,3] Aaron G. Rappaport,[1] Chris D. Muzny,[1] Dale W. Schaefer,[4] and Larry Hrubesh[5]

[1]*Condensed Matter Laboratory, Department of Physics, University of Colorado, Boulder, Colorado 80309*
[2]*Dipartimento di Elettronica, Universitá di Pavia, 27100 Pavia, Italy*
[3]*Exxon Research and Engineering, Annandale, New Jersey 08801*
[4]*Sandia National Laboratories, Albuquerque, New Mexico 87185*
[5]*Lawrence Livermore Laboratory, Livermore, California 94551*
(Received 22 April 1993)

We have studied, via x-ray scattering, the nematic to smectic-A (NA) translational ordering of the liquid-crystal-forming compound octylcyanobiphenyl (8CB) incorporated into the pores of a silica aerogel. We find that the aerogel dramatically alters 8CB phase behavior, eliminating the NA transition found at $T=T_{NA}=33.7\,^{\circ}$C in bulk samples and replacing it by a short range smectic ordering having a correlation length which at T_{NA} is $\xi\sim 40$ Å, much smaller than the aerogel pore and nematic domain size $\xi_p\sim 200$ Å. As T is lowered this smectic disorder is eliminated from the pores, ξ increasing continuously over a 20 °C range to saturate at ξ_p for $T<T_{NA}-20\,^{\circ}$C.

PACS numbers: 64.70.Md, 61.10.Lx, 61.30.Eb, 82.70.Gg

Understanding phase behavior in the presence of externally induced disorder is an area of current interest in statistical physics. Liquid crystals (LCs) offer unique opportunities in this context, a result of rather weak orientational and translational ordering which can be strongly influenced by surface interactions and which tend to be accompanied by long range correlations near phase transitions [1]. Silica aerogels, highly porous solids formed by aggregation and dehydration of suspensions of nm dimension silica particles, are attractive as hosts. The pores form a continuously connected volume which can occupy a volume fraction ϕ approaching unity ($\phi=0.79$ in the present case). The aerogel solid surface locally fixes LC molecular orientation and position, directly influencing its orientational and translational order parameters. Because these are nonconserved and the LC is a one component material it is not necessary to consider nonlocal effects such as phase separation. A particularly interesting LC phase transition is the nematic to smectic A, at which the orientationally ordered nematic (mean molecular long axis $\mathbf{n}$) becomes modulated by a one-dimensional (1D) density wave $\rho=\psi e^{i\mathbf{q}\cdot\mathbf{R}}$, describing the 2D-fluid layer stacking structure of the smectic A. Study of this transition in the pores of an aerogel offers the opportunity to probe the effects of induced disorder on a translational phase transition which is second order or weakly first order in the bulk.

The order parameter of the nematic-smectic-A (NA) transition can be chosen to be the complex 1D density wave amplitude $\psi=|\psi|e^{i\phi}$ which, as pointed out by de Gennes [2] and McMillan [3], enables a description of smectic-A ordering which is analogous to that of the appearance of superconductivity. For the smectic-A phase $|\psi|$ gives the magnitude of the density modulation and the phase $\phi(\mathbf{R})=\int_S[q(\mathbf{S})-\mathbf{q}_{0A}]\cdot d\mathbf{S}$, where $\mathbf{q}_{0A}=\hat{\mathbf{z}}2\pi/d_{0A}$, d_{0A} is the equilibrium A phase layer spacing, and $\hat{\mathbf{z}}$ is the layer normal. In equilibrium $\hat{\mathbf{n}}=\hat{\mathbf{z}}$ and $\phi=0$. Bulk 8CB exhibits isotropic (I), nematic (N), smectic-A (A), and crystal (X) phases as follows [4–6]: I ($T_{IN}=40.5\,^{\circ}$C) N ($T_{NA}=33.7\,^{\circ}$C) A ($T_{AX}=21.5\,^{\circ}$C) X. The NA transition is second order [7–9], or possibly very weakly first order [10,11], at which the specific heat exhibits a λ-like anomaly [6] and the nematic phase exhibits divergent pretransitional short range smectic ordering [5].

The aerogel used here, made by base-catalyzed hydrolysis and condensation of tetramethoxysilane [12], has a mass density $\rho=0.36$ g/cm^3. Debye-Anderson-Brumberger [13] and Porod [14] analyses of small angle x-ray scattering data [15] show a mean solid chord length of ~ 45 Å and pore size (void chord length) of $\xi_p\sim 200$ Å, respectively, void volume fraction of $\phi=0.79$, solid phase density of $\rho_s=1.75$ g/cm^3, and void surface to volume ratio $R_{SV}=0.024$ Å^{-1}. The 8CB-aerogel samples were prepared under vacuum using capillary action in the nematic phase to fill 0.5 and 1 mm thick slabs of aerogel, obtaining in this way a very slow filling that leaves the silica aerogel structure intact.

The phase behavior of these 8CB-aerogel samples has been studied by light scattering and precision calorimetry [16]. Turbidity measurements show that ξ_n, the correlation length for *nematic* ordering increases continuously, saturating at $\xi_n\sim 180$ Å for $T<36\,^{\circ}$C, comparable to the measured aerogel pore sizes noted above, with a local nematic orientational order parameter increasing smoothly with decreasing T, as in bulk 8CB. The heat capacity C_p of the 8CB aerogel showed hardly any trace of the distinct λ-like anomaly characteristic of the bulk NA transition, with C_p exhibiting a small excess over the expected IN contribution, appearing over the broad temperature range $15<T<32\,^{\circ}$C [16]. This suggests that the aerogel confinement strongly affects the NA transition.

0031-9007/93/71(21)/3505(4)$06.00

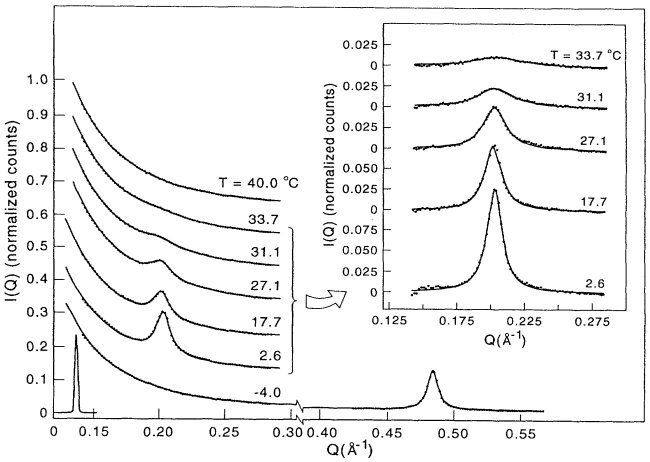

FIG. 1. X-ray scattering intensity $I(Q)$ from 0.36 g/cm^3 silica aerogel-8CB composite vs temperature. For clarity, each $I(Q)$ is shifted up relative to that of the next lowest temperature by 0.1 vertical unit. The smectic-A layering peak at 0.198 Å^{-1} narrows gradually in Q with decreasing temperature, abruptly disappearing at $T\sim 0\,^\circ$C to be replaced by crystalline peaks for Q in the range 0.48 Å$^{-1} < Q < 1.40$ Å^{-1}, with the peak at lowest Q ($q_x = 0.48$ Å^{-1}) having the largest intensity. The solid lines are fits by a sum of a Lorentzian (8CB) peak and a power-law (aerogel) background, with the $T = -4\,^\circ$C curve having only the power-law scattering. The inset shows the data and fits with the aerogel background subtracted. The count-rate normalization is such that 1 vertical unit $\sim 10^5$ counts/sec.

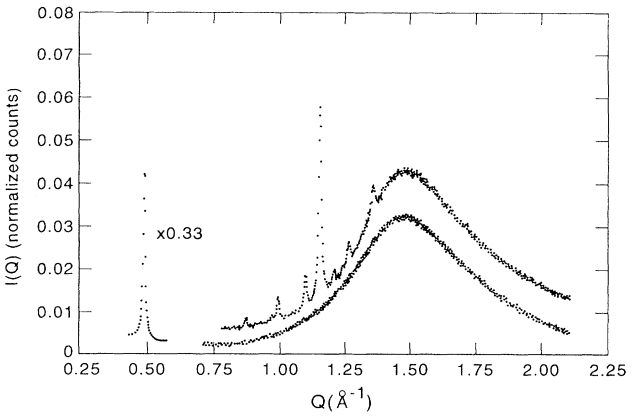

FIG. 2. X-ray scattering intensity $I(Q)$ for larger Q, showing only a broad scattering bump from the silica aerogel in the smectic-A phase ($T = 15\,^\circ$C) and an additional series of peaks from the 8CB in the crystalline phase ($T = -4\,^\circ$C). The aerogel background was fit by a polynomial and subtracted out and the two largest 8CB peaks fit to Lorentzians, yielding coherence lengths, $\xi_x = 255$ Å at $q_x = 0.484$ Å^{-1} and $\xi_x = 254$ Å at $q_x = 1.148$ Å^{-1}. Because of the overlap with each other and the background, ξ from the smaller peaks could not be reliably obtained, but fits gave ξ's comparable to those of the large peaks.

In order to directly probe the effects of the confinement on the NA transition, the x-ray structure factors $S(Q)$ of the aerogel and 8CB-aerogel system were measured using the diffractometer beam line X10B at the National Synchrotron Light Source at Brookhaven. The incident wavelength was 1.547 Å and the angular resolution $R(Q)$, shown in Fig. 1, was determined by slits in scattering angle 2θ at the detector to have a full width at half maximum of $\Delta Q \approx 0.003$ Å^{-1}. The transverse resolution, also determined by slits, makes no observable contribution to the line shapes. Samples were 1 mm thick slabs [16] mounted in a temperature controlled oven. Figure 1 shows the evolution vs T of the measured scattered x-ray intensity, $I(Q) \equiv R(Q) \otimes S(Q)$, for the filled aerogel, where $\otimes$ denotes convolution. The aerogel background scattering decreases monotonically with Q and, as the temperature is lowered in the nematic toward the bulk NA transition temperature, a diffuse scattering peak near $Q = q_{0A} = 0.198$ Å^{-1}, the wave vector of the bulk smectic layering in 8CB [5], appears in $I(Q)$, smoothly becoming narrower and more intense as the temperature is decreased. At $T\sim -2\,^\circ$C to $-5\,^\circ$C this smectic-A layering peak abruptly disappears, being replaced by the series of crystalline 8CB reflections shown in Figs. 1 and 2 for Q in the range 0.48 Å$^{-1} < Q < 1.40$ Å^{-1}. These peaks are much broader in Q than $R(Q)$ (see, for example, the peak at $Q = 0.484$ Å^{-1} in Fig. 1), indicating a finite range for crystalline order in the aerogel. Since bulk 8CB crystallizes at $T\sim 15\,^\circ$C, confinement in the aerogel suppresses crystallization, as is generally found for other first order crystallization transitions in porous media [17]. There are no crystal peaks for $Q < 0.48$ Å^{-1}.

The observable broadening of the peaks in Figs. 1 and 2 shows that long range translational order does not occur in 8CB in the aerogel in any part of the T range studied. Since the aerogel-8CB system is macroscopically isotropic, the scattering is a powder average over an isotropic distribution of short range ordered clusters. In this case $S_p(Q)$, the powder averaged $S(\mathbf{Q})$ for a peak at $\mathbf{q}_0$, may be written

$$S_p(Q) = \int d^3\mathbf{R}\, G(\mathbf{R}) [\sin(QR)/QR] \exp(-i\mathbf{q}_0 \cdot \mathbf{z}) ,$$

where $G(\mathbf{R})$ is the pair correlation function for the density wave amplitude,

$$G(\mathbf{R}) = \langle |\psi(0)||\psi(\mathbf{R})| \exp\{i\mathbf{Q}\cdot\hat{\mathbf{z}}[u(0) - u(\mathbf{R})]\} \rangle ,$$

and $u(\mathbf{R})$ is layer displacement along the layer normal [18]. A variety of functional forms for $S_p(Q)$ were used in attempts to fit the layering peaks in $I(Q)$, including powers of Lorentzians $S_p(Q) = AL(Q, q_0, \xi)^x \equiv A[1 + (Q - q_0)^2 \xi^2]^{-x}$, with $x = 0.5$, 2, etc. The simple Lorentzian ($x = 1$) gave the best fits in both the A and X phases.

Figure 2 shows the Bragg peaks in the range where the scattering vector has some component due to in-plane molecular spacings. The broad maximum is due to the aerogel silica [19]. In order to quantitatively character-

ize the spatial characteristics of the 8CB crystalline order, the silica background scattering was fit by a polynomial for $0.75\ \text{Å}^{-1} < Q < 2.00\ \text{Å}^{-1}$ and subtracted out. The two intense crystal peaks in Figs. 1 and 2 could then be reliably fit and fit well by $S_p(Q) \propto R(Q) \otimes L(Q, q_x, \xi_x)$; cf. the peak at $Q = q_x = 0.484\ \text{Å}^{-1}$ in Fig. 1, yielding the coherence lengths $\xi_x = 255$ Å at $q_x = 0.484\ \text{Å}^{-1}$ and $\xi_x = 254$ Å at $q_x = 1.148\ \text{Å}^{-1}$. The lack of Q dependence of ξ_x indicates single crystallites with a mean dimension ξ_x, essentially filling the aerogel pores.

The line shapes of all the crystal peaks were Lorentzian: $S_p(Q) = AL(Q, q_0, \xi_x)$. In this case, if we assume an isotropic $G(\mathbf{R})$, the susceptibility will be Lorentzian squared,

$$\langle |\psi(\mathbf{q})|^2 \rangle = \int d^3R\, G(\mathbf{R}) \exp(-i[\mathbf{q}\cdot\mathbf{R}]) \propto [1 + q^2\xi_x^2]^{-2},$$

and $G(\mathbf{R}) = A \exp[-R/\xi_x]$, a *simple* exponential. $G(\mathbf{R})$ can be interpreted in terms of finite size effects arising from the aerogel-induced disorder. In the limit that ξ is saturated at the pore size, $G(\mathbf{R})$ can be calculated using the arguments of Refs. [13] and [14] which give the Porod structure factor $[P(q) = (1 + q^2\xi_p^2)^{-2}$, q^{-4} at large $q]$ for the aerogel itself. We assume scatterers (the pores) modulated by a density wave of wave vector $\mathbf{q}_0$, which is uncorrelated in phase and orientation between separate pores, but bounded abruptly by randomly occurring surfaces [13,14]; then $G(\mathbf{R})$ has the simple exponential form and $\langle |\psi(\mathbf{q})|^2 \rangle$ has the square Lorentzian form above. Thus the Lorentzian shape for $I_p(Q)$ in both the X and saturated A phases is consistent with the Porod-like scattering found from the aerogel itself, discussed below.

Slow temperature scanning through the AX transition in the aerogel shows coexistence of the smectic-A and crystal peaks, with exchange of intensity without change of peak shape [20], indicating that for the strongly first order AX transition, a pore is either smectic A or crystal, in contrast to the nematic–smectic-A case, which we now discuss.

In order to characterize the short range smecticlike ordering of 8CB in the aerogel we first determined the shape of the background aerogel scattering in the Q range $0.12\ \text{Å}^{-1} < Q < 0.30\ \text{Å}^{-1}$ at the lowest temperatures where there is no smectic-A peak. Thus, for example, the $T = -4.0\,^\circ\text{C}$ scan in Fig. 1 $I(Q)$ was fit well by a power law plus a constant background: $I_b(Q) \sim a + bQ^{-\kappa}$, obtaining $\kappa = 3.68$, which was independent of temperature. This nearly Q^{-4} (Porod) dependence indicates that on length scales in this range the pore surface is nearly two dimensional. At the intermediate temperatures κ was fixed at 3.68 and the smectic peak $S_p(Q)$ taken to be a Lorentzian: $I(Q) = C + BQ^{-\kappa} + I_p(Q)$, with $I_p(Q) = A\{R(Q) \otimes L(Q, q_{0A}, \xi)\}$, and fit with C, B, A, ξ, and q_{0A} as adjustable parameters with the results shown in Fig. 1. We find $q_{0A} = 0.198\ \text{Å}^{-1}$, independent of T, the bulk value [5,6]. The resulting coherence length for smectic ordering, $\xi(T)$, is shown vs T in Fig. 3(a), along with the smectic layering correlation lengths in the bulk nematic, $\xi_\parallel$ and $\xi_\perp$ (---), which diverge as $T \to T_{NA}$. For $T > 35\,^\circ\text{C}$ $\xi(T)$ lies between $\xi_\parallel$ and $\xi_\perp$ but, as T approaches T_{NA}, does not diverge, reaching only $\xi \sim 40$ Å at $T = T_{NA}$. Instead, it increases smoothly with decreasing T over the range $20 < T < 35\,^\circ\text{C}$, asymptotically approaching $\xi = \xi_{\text{sat}} = 216$ Å at low T, clearly smaller than that achieved by the crystal phase (open circle). $\xi(T)$ is reversible for the rates of temperature change ($< 0.3\,^\circ\text{C/min}$) employed. The fits with the background subtracted in Fig. 1(b) show that there are small systematic deviations from the Lorentzian shape which are similar for the various temperatures.

Figure 3(b) presents $F(T) = \int I_p(Q,T)dQ/I_{\text{sat}}$, the intensity of the smectic layering peak integrated over the range $0.15\ \text{Å}^{-1} < Q < 0.275\ \text{Å}^{-1}$ and normalized by I_{sat}, its saturation value at low T for the aerogel. From $G(\mathbf{R})$ above we have that

$$F(T) \propto G(0) = \langle |\psi(\mathbf{R})|^2 \rangle = [1/V] \int_V d^3R |\psi(\mathbf{R})|^2,$$

thus giving a direct measure of the spatial average of the smectic order parameter $|\psi(\mathbf{R})|^2$ over V, the volume

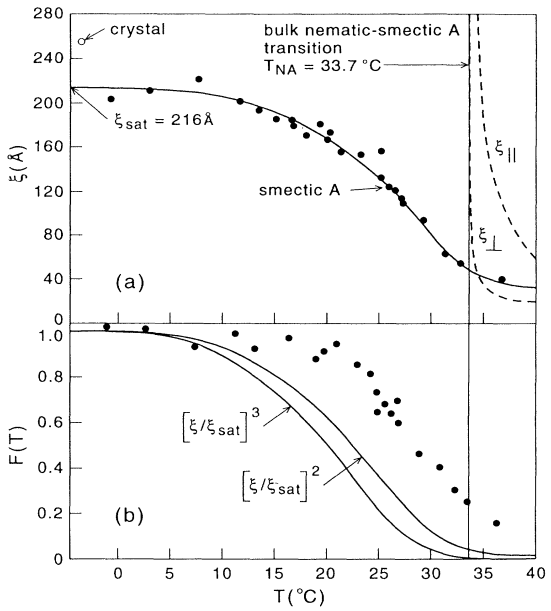

FIG. 3. (a) Correlation lengths for ordering of smectic layering in aerogel (●); of crystal layering in aerogel (○); and of smectic layering in bulk nematic (------) along $\hat{\mathbf{n}}$ ($\xi_\parallel$) and normal to $\hat{\mathbf{n}}$ ($\xi_\perp$). In the aerogel, at the bulk NA transition temperature, $T_{NA} = 33.7\,^\circ\text{C}$, the smectic-$A$ layering correlation length is only ~ 40 Å, increasing to $\xi_{\text{sat}} \sim 216$ Å, comparable to the pore size ξ_p, at low T. The solid line is a guide to the eye. (b) $F(T)$, the integrated smectic-A peak intensity normalized to its low T value. Also plotted are $[\xi(T)/\xi_{\text{sat}}]^2$ and $[\xi(T)/\xi_{\text{sat}}]^3$, which decrease much more rapidly with increasing T than $F(T)$, indicating that the growth behavior of the smectic layering is not type I.

filled by 8CB. The data show that in the aerogel $\langle|\psi(\mathbf{R})|^2\rangle$ increases smoothly with decreasing T, saturating at about 20 °C.

We interpret the smectic ordering results as follows. The data show that the smectic A can develop only short range order, up to the aerogel pore size, saturating at $\xi_{sat}=216$ Å even 35 °C below the bulk NA transition. This particular asymptotic limit at low T is not surprising in view of the fact that the smectic grows into a nematic that has only short range order ($\xi_n\sim 180$ Å, as noted above). What is remarkable is that at T_{NA}, where the bulk smectic orders, ξ in the aerogel has grown only to ~ 40 Å. This and the wide temperature range below the bulk T_{NA} in which ξ is much smaller than the pore size indicate the presence of a disordering mechanism operating on the length scale of 40 Å or smaller. Since the host nematic is ordered within the pores and the nematic light scattering shows no change through the smectic ordering process, indicating that smectic ordering does not affect the nematic correlations, it must be that smectic disorder is induced by the surfaces. The consequences of surface-induced smectic disorder can be obtained in two limiting scenarios, based on de Gennes' distinction between types I and II behavior in the smectic-A–superconductor analogy. In the type I scenario the smectic A will grow first where the nematic order parameter is largest. This will be in the space furthest away from the pore surfaces which we know to be disordering since both the IN and NA ordering are shifted to lower temperatures. Thus in the type I scenario the smectic A will form in drop or tubelike structures of dimension $\xi(T)$, and $F(T)$ would exhibit, respectively, $|\psi(T)|^2[\xi(T)/\xi_{sat}]^2$ and $|\psi(T)|^2\times[\xi(T)/\xi_{sat}]^3$ dependence in the two cases. Figure 3 shows that $F(T)$ grows much more slowly than either $[\xi(T)/\xi_{sat}]^2$ or $[\xi(T)/\xi_{sat}]^3$ alone, eliminating the type I scenarios, since the bulk $|\psi(T)|^2$ must also increase with decreasing T.

In the type II scenario the smectic order fills the nematic ordered pores, but with a disordered pinning of the phase of ψ at the pore surfaces, requiring vortex lines in ψ, smectic-A topological (edge and screw dislocation) defects. These surface-induced defect lines emanate from the surfaces and thermally equilibrate in the pores with a density that depends on $|\psi|^2$. As the temperature is lowered and the smectic order parameter grows, the defects become energetically more costly and are squeezed out to the surface of the pores. Away from the critical region ($T<30$ °C) $F(T)$ principally reflects the bulk behavior of $\langle|\psi|^2\rangle$, with perhaps some additional T dependence due to the reduction of smectic order in the defect cores. Where $F(T)$ and $\xi(T)$ are saturated ($T<15$ °C) it is reasonable to assume that smectic order has its bulk value everywhere, showing that the smectic order parameter is substantial throughout the T range up to T_{NA} where ξ is increasing and that a defect line picture of the interpore smectic disorder is appropriate. The nearly Lorentzian shape of $I_p(Q)$ for 15 °C $<T<$ 33 °C, where ξ becomes much smaller than the pore size, indicates that $G(R)$ may also be simple exponential within the pores when ξ is determined by vortex lines in the smectic order parameter. A theoretical analysis of $G(R)$ of this case would be very useful. The temperature range over which ξ grows is comparable to that over which the excess heat capacity attributable to smectic ordering is observed [16].

We acknowledge useful conversations with C. Safinya, M. Gingras, D. Huse, and C. Garland. This work was supported by NSF Solid State Chemistry Grant No. DMR 92-23729 to N.A.C. and a NATO Grant to T.B.

[1] P. S. Pershan, *The Structure of Liquid Crystal Phases* (World Scientific, Singapore, 1988).
[2] P. G. de Gennes, Solid State Commun. **10**, 753 (1972).
[3] W. L. McMillan, Phys. Rev. A **4**, 1238 (1971).
[4] P. P. Karat and N. V. Madhusudana, Mol. Cryst. Liq. Cryst. **36**, 51 (1976).
[5] D. Davidov, C. R. Safinya, M. Kaplan, R. Schaetzing, R. J. Birgenau, and J. D. Litster, Phys. Rev. B **19**, 1657 (1979).
[6] G. B. Kasting, C. W. Garland, and K. J. Lushington, J. Phys. (Paris) **41**, 879 (1980); J. Thoen, H. Marynissen, and W. Van Dael, Phys. Rev. A **26**, 2886 (1982).
[7] K. K. Chan, M. Deutsch, B. M. Ocko, P. S. Pershan, and L. B. Sorensen, Phys. Rev. Lett. **54**, 920 (1985).
[8] M. R. Fisch, P. S. Pershan, and L. B. Sorensen, Phys. Rev. A **29**, 2741 (1984).
[9] L. Ricard and J. Prost, J. Phys. (Paris) **42**, 861 (1981).
[10] M. A. Anisimov, P. E. Cladis, E. E. Gorodetskii, D. A. Huse, V. E. Podneks, V. G. Taratuta, W. van Sarloos, and V. P. Voronov, Phys. Rev. A **41**, 6749 (1990).
[11] M. Benzekri, T. Claverie, J. P. Marcerou, and J. C. Rouillon, Phys. Rev. Lett. **68**, 2480 (1992).
[12] D. W. Schaefer, J. P. Wilcoxson, K. D. Keefer, B. C. Bunker, R. K. Pearson, I. M. Thomas, and D. E. Miller, in *Physics and Chemistry of Porous Media II*, edited by J. R. Banavar, J. Koplik, and K. W. Winkler, AIP Conf. Proc. No. 154 (AIP, New York, 1987), p. 63.
[13] P. Debye, H. R. Anderson, and H. Brumberger, J. Appl. Phys. **28**, 679 (1957).
[14] G. Porod, in *Small Angle X-Ray Scattering*, edited by O. Glatter and O. Kratky (Academic, New York, 1982).
[15] D. W. Schaefer and K. D. Keefer, Phys. Rev. Lett. **56**, 2199 (1986); D. W. Schaefer, J. Phys. (Paris), Colloq. **24**, C4-121 (1989).
[16] T. Bellini, N. A. Clark, L. Wu, C. W. Garland, D. Schaefer, and B. Olivier, Phys. Rev. Lett. **69**, 788 (1992).
[17] J. Warnock, D. D. Awschalom, and M. W. Shafer, Phys. Rev. Lett. **57**, 1753 (1986).
[18] C. R. Safinya, D. Roux, G. S. Smith, S. K. Sinha, P. Dimon, N. A. Clark, and A. M. Bellocq, Phys. Rev. Lett. **57**, 2718 (1986).
[19] G. Reichenauer, U. Buchenau, and J. Fricke, Rev. Phys. Appl. Colloq. **24**, C4-145 (1989).
[20] A. G. Rappaport, B. Thomas, T. Bellini, and N. A. Clark (to be published).